Caspian Journal of Environmental Sciences
Online ISSN: 1735-3866
Print ISSN: 1735-3033

Monitoring the spatial changes of river water quality through the fusion of Landsat 8 images and statistical models (A case study: Sefidroud River, Northwest Iran)

Yosef pourhabib[1], Ebrahim Fataei[1]*, Fatemeh Nasehi[1], Behnam Khanizadeh[2], Hossein Saadati[1]

1. Department of Environmental Sciences and Engineering, Ardabil Branch, Islamic Azad University, Ardabil, Iran
2. Department of Chemistry, Sarab Branch, Islamic Azad University, Sarab, Iran

* *Corresponding author's E-mail: eb.fataei @iau.ac.ir*

ABSTRACT
The present study determined the relationship between spectral reflectance of satellite images and water quality parameters (WQPs) to monitor water quality of Sefidroud River in Northwest Iran. The data of 12 WQPs were obtained from the regional water department in four hydrometric stations during 2013-2018. Principal component analysis (PCA) was used to reduce the number of WQPs. After pre-processing 19 Landsat 8 images simultaneously with WQPs sampling and fusing panchromatic band with spectral bands and increasing the band resolution to 15 × 15 m, the findings were employed to determine the relationship between spectral reflectance and band ratios. The PCA results revealed that Sum A (sum of anions), Sum C (sum of cations), TDS and EC were in the first principal component and HCO_3^- in the second principal component. The relationship of these five WQPs was statistically investigated with seven single spectral bands and 21 band ratios using regression models and curve estimation, thereby choosing the best regression model. Sum A, TDS and EC was correlated with band 5, Sum C with band ratio 4/3, and HCO_3^- with band 6 (R = 70%). Mapping spatial changes in WQPs using regression models and spectral data indicated higher values in the upstream areas prior to Manjil Dam, decreased values in the dam inflow, while increased those in its outflow. The research results highlighted the usefulness of Landsat 8 images for water quality monitoring.

Keywords: Factor analysis, Landsat 8, Sefidroud River, Water quality, WQPs.
Article type: Research Article.

INTRODUCTION
Water quality is defined based on chemical, physical and biological attributes (especially bacteriological) of water, which may be different for various regions on the basis of topography, land use, land cover and climatic factors (Shukla *et al.* 2018). The change in surface water quality forms a new ecological environment that is different from the original one, in fact a different biological environment based on the adaptation of aquatic organisms to the new environment (Luo *et al.* 2020). On the other hand, the interaction between land use and river system is more complicated in basins with extensive anthropogenic activities, such as the presence of numerous dams and valves. The water stored behind the dams and valves leads to changes in the flow and self-purification capacity of rivers (Gu *et al.* 2019). Therefore, pollutants remain in the river for a long time and affect its ecosystem in comparison with basins without dams and valves. Thus, the seasonal effects of water quality and water ecology may be greater in such basins (Luo *et al.* 2020). Since 1990, although water quality plays an important role in the industrial, agricultural and public health sectors, extensive anthropogenic activities around the world have led to a decrease in water quality. Reportedly, the water pollution has worsened in most rivers of Latin America, Africa and Asia (Yadav *et al.* 2019). Many rivers worldwide are reportedly losing their water quality (Kändler *et al.*

Caspian Journal of Environmental Sciences, Vol. 23 No. 2 pp. 315-326 Received: June 05, 2024 Revised: Sep. 11, 2024 Accepted: Nov. 20, 2024
DOI: 10.22124/CJES.2025.8685

Publisher: University of Guilan,

2017; Cerqueira *et al.* 2020; Zhang *et al.* 2021). In recent years, many aquatic ecosystems suffer from high levels of terrestrial pollutant loads due to anthropogenic activities (urban, industrial and agricultural) combined with natural processes (rainfall inputs, erosion and seasonal effects). As a result, the quality of water resources has deteriorated, biodiversity has decreased, and the health of the river ecosystem has been threatened. Hence, it is vital to protect fresh water sources and identify factors affecting river water quality (Tian *et al.* 2019). On the other hand, water demand is increasing at the rate of 1% per year at the global level, and this amount is expected to intensify in countries with developing and emerging economies (Yadav *et al.* 2019). Since pollution reduces the usable water supply of any region, places where the available water resources are insufficient to meet the ever-increasing water demand suffer from water scarcity. Therefore, water quality monitoring and assessment play a prominent role in the protection of natural ecosystems, public health, agriculture and industry (Zhang *et al.* 2021). Recently, successive droughts as well as population growth and increasing water demand have put Iran in a crisis stage. The most basic solution to circumvent this bottleneck (water stress in the country) is the proper management of the country's water resources, which is possible by obtaining comprehensive and accurate data (Hashemifard *et al.* 2018). The techniques used in this field, including Remote Sensing (RS) and Geospatial Information System (GIS), have not been limited to some specific fields, and have played a key role in environmental planning, development and management (Mishra *et al.* 2021). The relationship between the spectral behavior of water and its optically active components (OAC) has made remote sensing and digital image processing a valuable tool for monitoring water quality. The interaction between solar radiation and OAC changes the spectral characteristics of water and therefore can be used as an indicator of water quality. Satellites such as Landsat 8 are expected to be calibrated to monitor water quality and provide good accuracy in the next 10 to 15 years (Pizani *et al.* 2020). Many studies in all parts of the world have used satellite spectral data to investigate water quality parameters (WQPs). A study investigated the correlation of Landsat 8 spectral bands and WQPs of the Nakdong River in Korea, and reported that band 5 had a significant correlation with all WQPs. The suspended solids (SS) and chlorophyll-a had a correlation of 74 and 71%, respectively (Lim & Choi 2015). In a study in a Himalayan lake in northwest Kashmir, the results showed that most WQPs had a correlation (R^2) up to 0.5 with the spectral data of Landsat 8 bands (Mushtaq *et al.* 2017). A study in Eastern Oklahoma in the south-central United States used Landsat 5 and 8 series images. The findings indicated that Shortwave Infrared (SWIR) bands had higher Pearson correlations with chlorophyll and water turbidity rather than other spectral bands (Clay Barrett & Frazier 2016). A study in Trichonida lake in Western Greece by examining the relationship between WQPs and Landsat 8 data concluded that correlation coefficient (R) was up to 0.7 and 0.5 for ammonium and chlorophyll-a concentrations, respectively (Markogianni *et al.* 2018). A study sampled the WQPs of Geshlagh reservoir in Kurdistan Province, Northwest Iran, reporting a correlation of water chemical variables including total nitrogen (TN) and total phosphorus (TP) concentrations with chlorophyll-a concentration using Landsat 8 Operational Land Imager (OLI) data, linear regression model and artificial neural network. The findings indicated the band ratio 3/2 and the single bands 3 and 4 as the most suitable bands for determining the concentration of chlorophyll-a in Geshlagh reservoir (Vakili & Amanollahi 2020). A study in Northeast Africa monitored the changes in chlorophyll-a concentration in Vaal Dam using Landsat 8 and Sentinel 2 dataset. The results showed that the blue-green band ratio in Landsat 8 and the infrared-to-red band ratio with R^2 values of 0.89 and 0.75 respectively were suitable indicators for chlorophyll-a retrieval (Obaid *et al.* 2021). A study in Northern India used data from seven water quality sampling stations to investigate Pearson's correlation and its variation with Landsat 8 Level 1 Surface Reflectance datasets exhibiting a correlation between variations in WQPs and average surface reflectance (Mishra *et al.* 2021). A research in the south and east coasts of Vietnam used Sentinel 2 data and the Random Forest (RF) model, reporting a correlation coefficient (R^2) of 0.7 between chlorophyll concentration and sea surface reflectance (Quang *et al.* 2023). The majority of studies on the relationships between spectral bands and WQPs have been focused on using statistical models of correlation and regression relationships, and have neglected to map the changes of WQIs. One of the innovations of the present research was to map the spatial changes of water quality parameters along the studied river, which not only made it possible to identify the more polluted areas, but also helped to identify possible pollution sources. When the resolution size of a specific phenomenon is much smaller than the resolution power of satellite images, the ability to discover and determine that phenomenon using satellite images will be problematic. In this case, the statistics generated from satellite images may lack significant details (Maynard *et al.* 2016). For example, many rivers in Iran are less than 30 m wide, hence using Landsat 8 images with 30 × 30-meter spectral bands cannot provide the possibility of separating the spectral reflectance of water. To overcome this problem, many researchers have used the fusion of satellite images. During this process, spatial information is extracted from images with high spatial resolution and spectral information is extracted from images with high spectral resolution. Subsequently, fusing them creates an image with high spatial and spectral accuracy. The fusion of data increases their usability, so that a new image with more comprehensive information can be accessed (Fensholt *et al.* 2010). Accordingly, the present study tried to improve the power and accuracy of the spatial resolution of the river water quality change map using the panchromatic band and the satellite image integration technique. We fused 30 × 30-meter spectral bands using Landsat 8 15 × 15-meter panchromatic band, and then analyzed statistical models for WQI and spectral bands to map the WQI changes in the Sefidroud (also called Sepidrood) River in the North Iran.

MATERIALS AND METHODS

Study area

Sefidroud basin is of the largest ones in Iran, a subset of the Caspian Sea basin. The area of this basin is 59,217 square kilometers (km^2), with its main river being the Sefidroud (Ghaffari *et al.* 2022). The river is formed by the joining of two rivers, Shahrood River (from the southeast side) and the Ghezel Ozan River (from the northwest side), beside Manjil City. It flows into the Caspian Sea at Bandare Kiashahr City after crossing the width of Guilan Province. Manjil dam is located on Sefidroud in Manjil City, which was put into operation in 1963 with an initial storage capacity of 1.76 billion cubic meters at the normal level of the reservoir. The mean annual discharge (MAD) of this river is 3998 million cubic meters. The river can irrigate many lands downstream due to the construction of Manjil Dam and other reservoir and diversion dams on it, which not only provides hydroelectric power, but also plays a vital role in livestock production, agriculture and fisheries. This study has used information from four regional hydrometric stations in Guilan, which collect water quality data. The Gilvan station is located on Ghezel Ozan River, the Lowshan station on Shahrood River, the Rudbar station on Sefidroud River after Manjil Dam, and the Astaneh-ye Ashrafiyeh station in Astaneh-ye Ashrafiyeh County close to the shores of the Caspian Sea on the Sefidroud River. Fig. 1 shows the location of four studied stations (Guilan Regional Water Authority, 2017).

Data analyzed in the study

The water quality of Sefidroud River was monitored using data collected between 2013 and 2018 from four hydrometric stations of Gilvan, Lowshan, Rudbar and Astaneh-ye Ashrafiyeh affiliated to Guilan Regional Water Authority (Guilan Regional Water Authority, 2017). These stations record data on WQPs, including calcium (Ca), magnesium (Mg), sodium (Na), potassium (K), chlorine (Cl), sulfate (SO_4^{2-}), bicarbonate (HCO_3^-), anion sum (Sum. A), cation sum (Sum. C), total dissolved solids (TDS), electrical conductivity (EC) and total hardness (TH). The quality control for qualitative parameter data in terms of outliers was done by SPSS software using homogeneity as well as randomness and independence tests based on the non-diagrammatic Run-Test method and the non-parametric Mann-Whitney U test, respectively. Finally, 19 samples of WQPs in the studied stations were used for analysis. The present research used the data of spectral bands of Level-1 Precision and Terrain (L1TP) Landsat 8 images. To this end, 19 images captured by the Operational Land Imager (OLI; path: 166, row: 34) between 2013 and 2018 were acquired from the United States Geological Survey (USGS). The images were extracted at the same time as the WQP samples were taken (on the same day), which were appropriate in terms of cloudiness and quality.

Satellite image preprocessing

After receiving the mentioned satellite images, the data quality was controlled based on atmospheric, geometric and radiometric errors using ENVI 5.3 program. Since the majority of received images had a coordinate system, there was no need for geometric correction. Radiometric correction was done for all received images. The atmospheric correction was performed using Fast Line-of-sight Atmospheric Analysis of Spectral Hypercubes (FLAASH) module to ensure accurate recovery of spectral information of images. The parameters required for the atmospheric correction were extracted from the MTL text file data as well as the Advanced Spaceborne Thermal Emission and Reflection Radiometer (ASTER) 30-meter DEM (Ansari & Akhoondzadeh 2020).

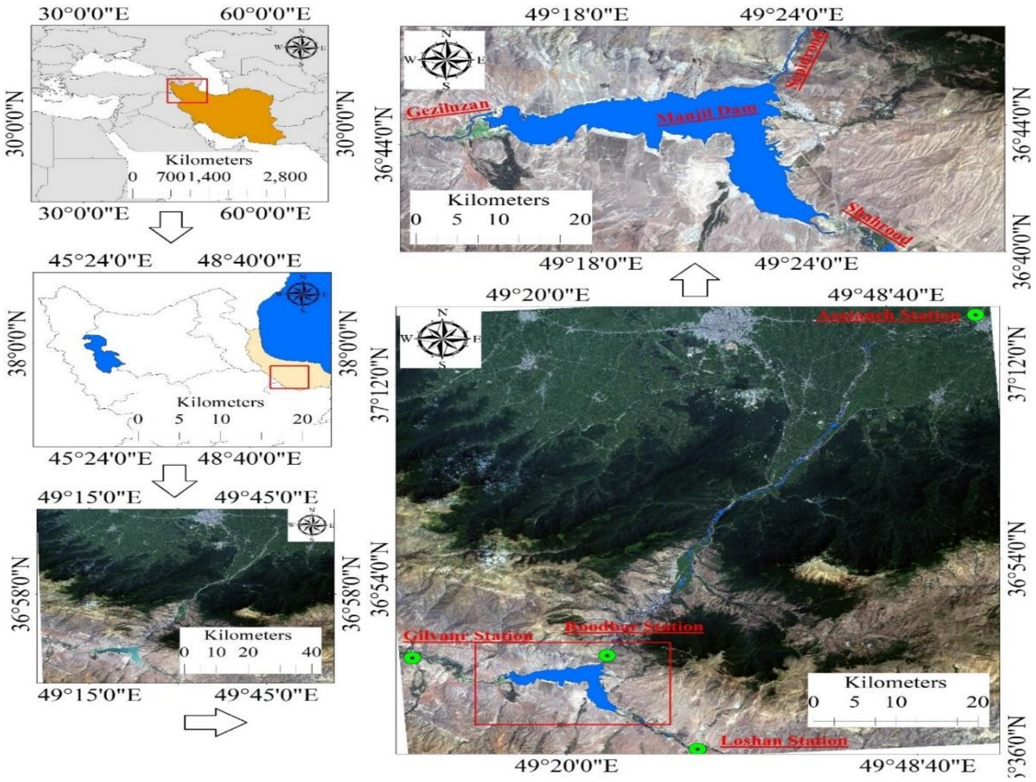

Fig. 1. Location of Sefidroud River and hydrometric stations under study, Guilan Province, Iran.

Fusion of images

Remote Sensing (RS) studies are more interested in pixel-level image fusion (Xu & Ehlers 2017). Pixel-based satellite image fusion algorithms use the geometric details of a high-resolution panchromatic (PAN) image and spectral information from a multispectral (MS) image with low spatial resolution to generate a high spatial resolution MS image (Zhang *et al.* 2016; Pushparaj & Hegde 2017). In recent years, many efforts have been made to provide algorithms suitable for fusing spectral and spatial data of satellite images (Im *et al.* 2008; Kavzoglu & Colkesen 2009; Yia *e al.* 2012). The current research used the Gram-Schmidt algorithm, in which a PAN band is simulated using the MS image spectral bands. Generally, in this algorithm, the simulated PAN band is obtained by averaging the MS image bands, and is considered as the first band. Then, the Gram-Schmidt transformation is conducted for the simulated PAN band and the MS bands. Next, the PAN band of the high-resolution image is replaced with the first Gram-Schmidt band (Liao *et al.* 2014; Sarp 2014).

Water zone separation

The Modified Normalized Difference Water Index (MNDWI) was used to delineate the water zone. The normalized difference water index (NDWI) has been designed to monitor plant water content and has been modified to MNDWI (Xu 2006) to better highlight the water information in Landsat bands. The MNDWI was calculated according to Equation 1.

$$MNDWI = \frac{Green+SWRI}{Greem-SWIR} \quad (1)$$

Statistical analysis

One of the multivariate statistical analysis methods is factor analysis (FA), which can be used to reduce the complexity of analyzing the primary variables of the problem in cases where we deal with a large amount of information and also for better interpretation of the information (Goodarzi *et al.* 2019). This research used the statistical model of principle component analysis (PCA) to determine factors (principle components) and reduce the number of plant indicators. The factors with the number of eigenvalues greater than one were considered to select the number of factors. The initial eigenvalues were estimated for each of the factors in the form of the sum of explained variance. The explained variance was a percentage of the total variance and cumulative percentage.

In fact, the eigenvalue of each factor was a proportion of the variance of all variables explained by that factor. The eigenvalue could be calculated through the sum of the squared factor loadings related to all the variables in that factor. Therefore, eigenvalue showed the exploratory importance of factors in relation to variables. The low value of this index for a factor meant that it had a small role in explaining the variance of the variables. The extracted values of the squared values were actually the explained variance of the presented factors whose eigenvalues were greater than one (Bihamta & Zare Chahouki 2015). Accordingly, the 12 studied WQPs were reduced to several factors (groups) and among the indicators belonging to each factor (group), the indicators with high weight were considered as the selected indicators of that group.

Correlation between spectral reflectance and WQPs

After choosing the appropriate WQPs, the relationship between changes in qualitative parameters and spectral reflectance was analyzed. In order to investigate the spectral reflectance of the runoff of Sefidroud, Ghezel Ozan and Shahrood rivers, first, five fixed 15-meter pixels were considered in all images from the location of the stations to 150 meters upstream of the station. Then, the average values of spectral reflectance of seven image bands were calculated in these five pixels. The average spectral reflectance of 5 fixed pixels at the closest point to the hydrometric stations was more suitable for checking the water quality compared to the spectral reflectance of one pixel. It was due to the possibility of errors caused by the geometric and radiometric attributes of the images. After extracting the spectral reflectance values of the image bands, the correlation between WQPs and spectral reflectance of 7 bands and 21 band ratios was investigated. In such studies, the criterion is usually the ratio of the larger band to the smaller one. A total of 28 spectral parameters including bands and band ratios were used to check the correlation between WQPs and spectral reflectance of the images. Curve Estimation was used to select the most suitable simple correlation equation using SPSS 21 and high correlation coefficients were considered as the criterion for choosing the most suitable equation.

Mapping the spatial variation of WQPs

After selecting the most suitable parameters and regression model, the satellite image data of 2016 was used to calculate and draw the map of spatial changes using the raster calculator tool in the ArcMap program. In that year, on the date of sampling for WQPs (July 30, 2016), the Sefidroud River was in a high flow state, with a water discharge of 289 $m^3 s^{-1}$. In addition, the analysis of prepared maps was used to investigate the changes of WQPs at the inflow of Ghezel Ozan and Shahrood rivers to Manjil Dam and Sefidroud River after leaving the dam at Rudbar and Astaneh-ye Ashrafiyeh stations.

RESULTS

Data fit for factor analysis

The test of homogeneity, randomness and independence of the data showed that all the data in question were homogeneous, random and independent. Since the FA method is based on the correlation between the variables, the correlation matrix between the variables should also be calculated using this method. In fact, the correlation matrix showed the existence of a relationship between some variables and its non-relationship with others. The results of Pearson's correlation matrix revealed a very strong correlation between the studied WQPs. The results of Kolmogorov–Smirnov test showed the normality of the data. All WQPs, except HCO_3^-, were correlated at the 1% probability level. Therefore, the high correlation coefficients of the indicators showed the fitness of the examined variables for factor analysis

Principal components analysis

Based on the PCA results, about 91% of the variation was related to the first two principal components, so that the first principal component (PC1) explained about 81% of the variance of the qualitative parameters under investigation. By adding 10% of the variance to the second principal component (PC2), a total of 91% of the variation was explained (Table 1). By rotating the factor components, PC1 and PC2 explained about 71% and 20% of the variation, respectively, and no significant changes were observed in the total variances. Due to the high weight of more variables, the criteria of 1 for PC1 and 0.94 for PC2 were considered as the numerical threshold for selecting variables (Table 2). Accordingly, TDS, EC, Sum A and Sum C were placed in PC1 and HCO_3^- in PC2.

Table 1. Results of factor analysis (eigenvalue and variance corresponding to factors) for 12 water quality parameters of Sefidroud River at studied hydrometric stations, Guilan Province, Iran.

Principal components	Initial Eigenvalues			Extraction Sums of Squared Loadings			Rotation Sums of Squared Loadings		
	Total	Rate of Variance (%)	Cumulative (%)	Total	Rate of Variance (%)	Cumulative (%)	Total	Rate of Variance (%)	Cumulative (%)
1	10.54	81.05	81.05	10.54	81.05	81.05	9.21	70.86	70.86
2	1.27	9.79	90.84	1.27	9.79	90.84	2.60	19.98	90.84
3	0.73	5.60	96.44	-	-	-	-	-	-

Table 2. Unrotated factor matrix for 12 water quality parameters of Sefidroud River at studied hydrometric stations, Guilan Province, Iran.

Water quality parameters	PC1	PC2
TDS	1.00	0.07
EC	1.00	0.07
SO_4^{2-}	0.86	-0.42
HCO_3^-	-0.22	0.78
Cl	0.96	0.23
Sum A	1.00	0.06
Ca	0.91	-0.25
Mg	0.84	-0.25
Na	0.96	0.23
K	0.86	0.17
Sum C	1.00	0.08
TH	0.93	-0.26

Regression model results for WQPs based on satellite images

The results of examining the highest correlation of 28 spectral parameters (including 7 bands and 21 band ratios) and 5 selected WQPs indicated that TDS, EC and Sum A had 74, 74 and 75% linear correlation with band 5, respectively. Sum C had 74% power correlation with Band 4/Band 3, while HCO_3- had 74% exponential correlation with Band 6 at 1% probability level (Table 4 and Fig. 2).

Map drawn for spatial variation of WQPs

Fig. 3 shows the map of spatial variation of Sum A, Sum C, TDS, EC and HCO_3^- in 2016. The changes of the Sum A varied between 7.5 and 7.6 mg L^{-1}, with an average value of 19.7 mg L^{-1}. The changes of the Sum C ranged from 7.5 to 7.6 mg L^{-1}, with an average value of 19.7 mg L^{-1}. The TDS value varied between 9.2 and 31.7 mg L^{-1}, with an average value of 14.9 mg L^{-1}. The value of EC varied from 786.9 to 7276.2 µs cm^{-1}, with an average value of 1984.5 µs cm^{-1}. The HCO_3^- concentration also varied between 0.4 and 3.1 mg L^{-1}, with an average value of 2.6 mg L^{-1}.

Table 4. The regression equations based on curve estimation of bands and band ratios for water quality parameters of Sefidroud River at studied hydrometric stations, Guilan Province, Iran.

Sig.	F	R-square	R	Regression equations	Type of equation	Spectral data	Parameters
	20.53	0.55	0.74	TDS = 11441(B5) + 415.56	Linear	Band 5	TDS
	20.53	0.55	0.74	EC = 18157(B5) + 659.78	Linear	Band 5	EC
0.01	20.53	0.56	0.75	Sum A = 184.96(B5) + 6.211	Linear	Band 5	Sum A
	17.37	0.55	0.74	Sum C = $19.78(B4/B3)^{1.392}$	Power	Band 4/Band 3	Sum C
	13.25	0.55	0.74	$HCO_3 = 2.2233e^{-2.392(B6)}$	Exponential	Band 6	HCO_3^-

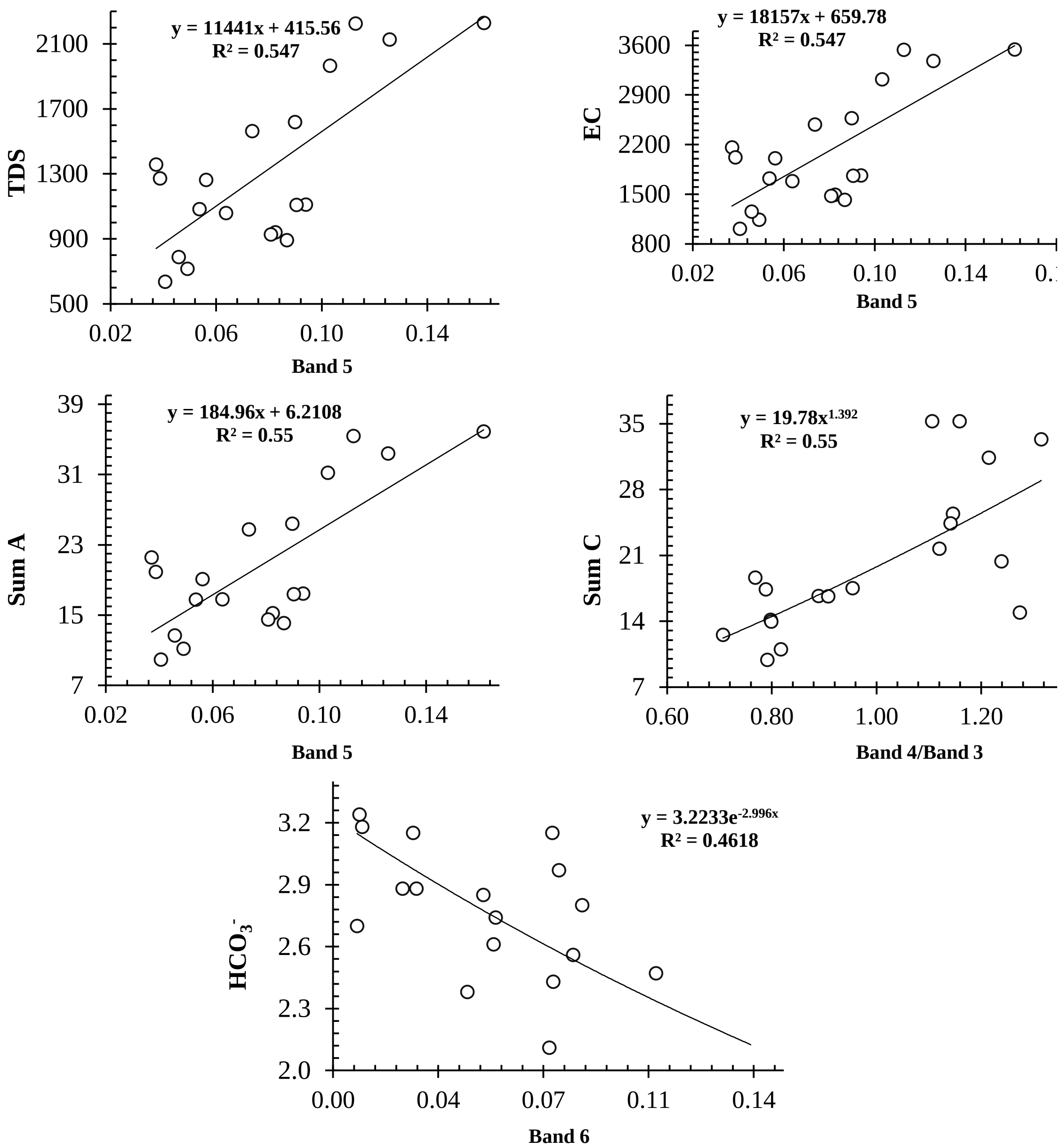

Fig. 2. Regression model based on spectral data of satellite images for water quality parameters of Sefidroud River at studied hydrometric stations, Guilan Province, Iran.

Fig. 4 shows the spatial changes of EC values at the inflow of Ghezel Ozan and Shahroud rivers to Manjil Dam and Sefidroud River after leaving the dam at Rudbar and Astaneh-ye Ashrafiyeh stations. As can be seen, the EC values in the inflow of Ghezel Ozan and Shahroud rivers to Manjil Dam were high, which decreased after entering the dam. The EC value at the outflow of Manjil Dam at Rudbar station was similar to that of Manjil Dam, but it increased as reached Astaneh-ye Ashrafiyeh station. The temperature values measured at the three stations during the study period (Fig. 2) ranged from 19.2 °C to 21.9 °C. At the end of spring, there was a remarkable increase in temperature. These temperature variations followed those of the regional climate. Indeed, the average seawater temperature is related to weather conditions as the surface layer is subjected to the direct influence of the regional climate characterized by a cold- and a warm- seasons (Chaouay *et al.* 2016).

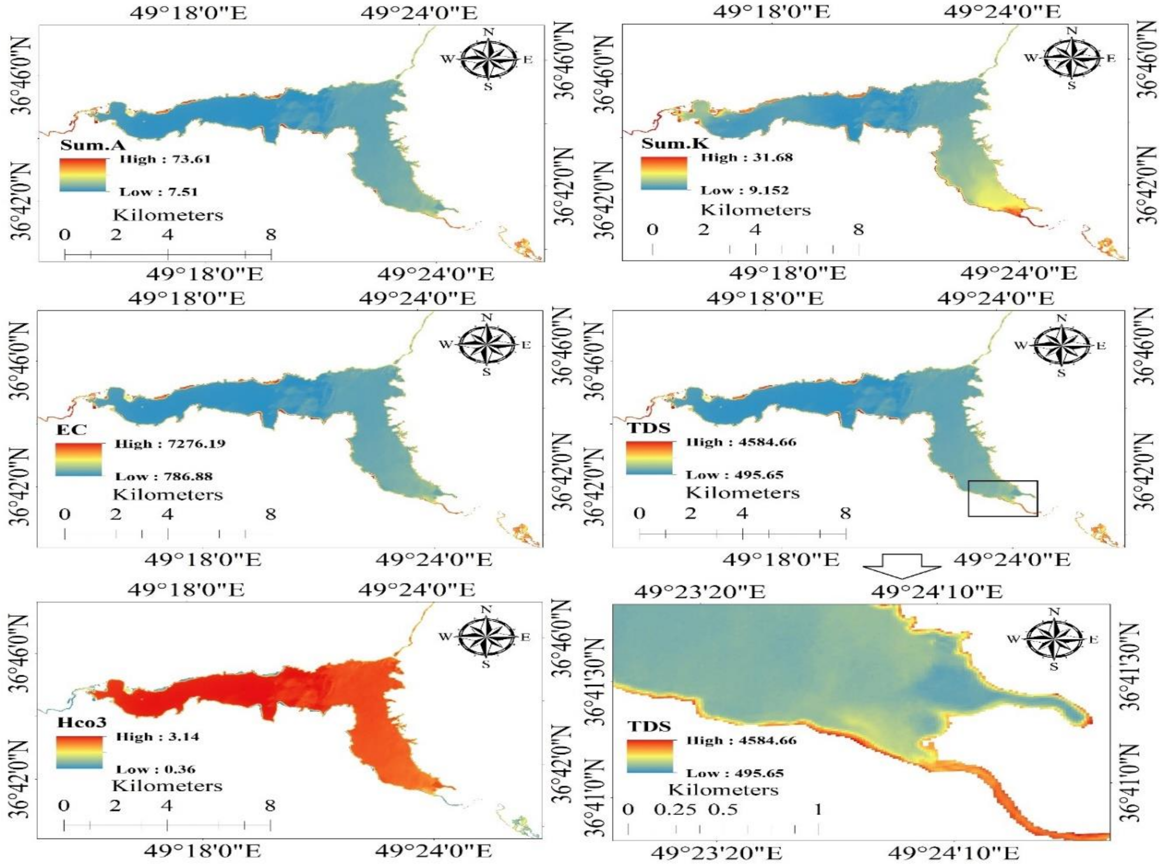

Fig. 3. Spatial changes of Sum A, Sum C, TDS, EC and HCO3- parameters in Sefidroud River at studied hydrometric stations, Guilan Province, Iran, July 20, 2016.

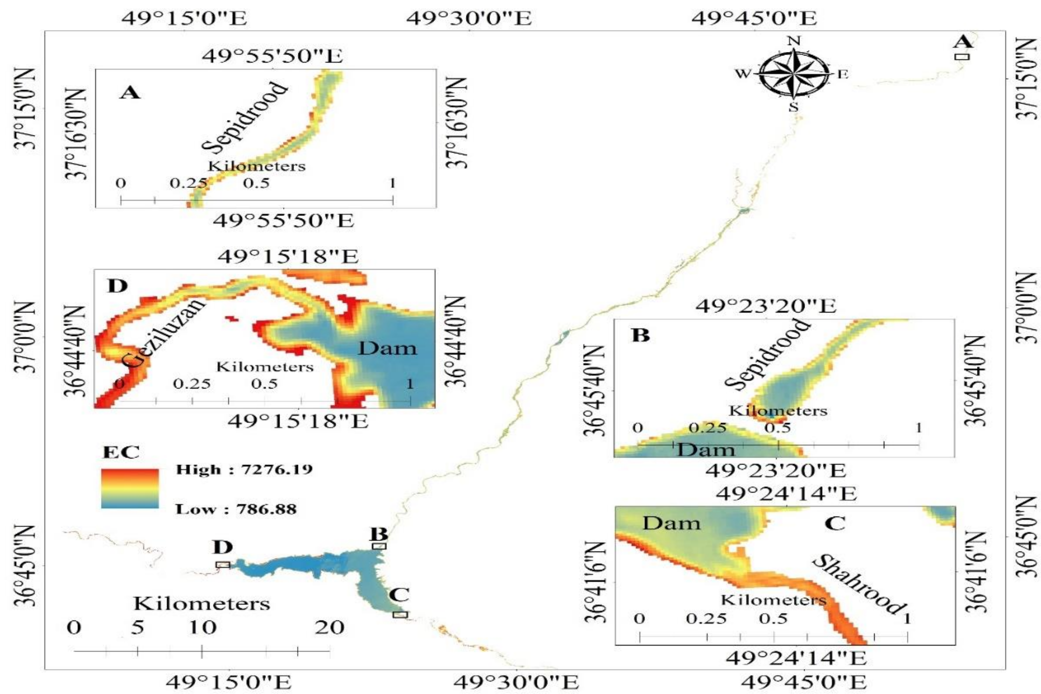

Fig. 4. Spatial changes of EC in outflow and inflow of Manjil Dam and Astaneh-ye Ashrafiyeh station on Sefidroud River, Guilan Province, Iran, July 20, 2016.

DISCUSSION

In this research, after pre-processing the Landsat 8 images and fusing the panchromatic band of 15 × 15 meters with 7 spectral bands of 30 × 30 meters, we obtained seven spectral bands with 15 × 15 accuracy. Then, the statistical analyzes were used to determine the relationship of water quality parameters, including Sum A, Sum C, TDS, EC and HCO_3^-, and spectral bands and band ratios. In general, the results indicated a relatively good correlation (R^2; up to 0.5) between WQPs and Landsat 8 spectral bands. The findings of many other studies, such as in northern India (Mishra *et al.* 2021) and in southern and eastern Vietnam (Quang *et al.* 2023), have pointed to the correlation between WQPs and the spectral bands of satellite images. According to the results of the regression equations, Sum A, TDS and EC exhibited correlation coefficients (R) above 74, 74 and 75 with band 5, respectively. This result was in accordance with other previous studies (Lim & Choi 2015; Mushtaq *et al.* 2017; Markogianni *et al.* 2018), as it was shown that all WQPs had a high correlation with band 5. The correlation coefficients of SS and chlorophyll-a were also 74 and 71, respectively (Lim & Choi 2015). In addition, it was found that the majority of WQPs had a correlation above 0.5 with Landsat 8 data (Mushtaq *et al.* 2017). Examining the relationship between Landsat 8 data and ammonium concentration resulted in a high correlation coefficient of 0.7 (Markogianni *et al.* 2018). In our study, Sum C also exhibited a 75% correlation with the band ratio of 4/3. This finding was similar to the results of Vakili & Amanollahi (2020), who reported the high correlation of single bands 3 and 4 with TN and PN. It has been shown that the band ratio of 4 to 3 had a high correlation (0.8) with the concentration of chlorophyll-a (Obaid *et al.* 2021). According to our results, the HCO_3^- concentration displayed a correlation of 0.55 with spectral values of band 6. This result was consistent with other studies (Clay Barrett & Frazier 2016; Jalalzadeh *et al.* 2022), who concluded that the SWIR band had a higher Pearson correlation with chlorophyll and water turbidity than other spectral bands. The optical properties of water are different due to different concentrations of quality parameters and different turbidity of water. In addition, the sensitivity of water spectral reflectance is often higher in the visible and near-infrared ranges. Therefore, GIS data can be considered as an effective solution to investigate water quality parameters, especially in the absence of sampling data in many regions of the world. After mapping the spatial changes of WQPs, the difference in concentration of parameters was investigated between the upstream and downstream areas of Sefidroud River. The results showed that the values of WQPs were high in the upstream areas at the inflow of Ghezel Ozan and Shahroud rivers to Manjil Dam, but they were reduced by discharging to Manjil Dam and also at the outflow of Manjil Dam at Rudbar station. The interaction between land use and the river system is more complicated in basins with extensive anthropogenic activities, such as the presence of numerous dams and valves (Gu *et al.* 2019, Safizadeh *et al.* 2021), so that water storage behind dams and valves leads to changes in the flow and self-purification capacity of rivers. Comparison of WQPs values at Manjanil Dam outflow site with Astaneh-ye Ashrafiyeh station at the most downstream studied point near the connection of Sefidroud to the Caspian Sea showed that WQPs values at Astaneh-ye Ashrafiyeh station were increased compared to Rudbar station. In fact, the path of Sefidroud River in this part of the study area passes through agricultural lands and urban residential areas, and it seemed that the values of WQPs had increased as a result of anthropogenic activities. The investigation about the effect of land use on water quality in the upper Nisa catchment in the Czech Republic and also in Germany revealed that watersheds with the predominant use of residential and agricultural areas had caused a decrease in water quality (Kändler *et al.* 2017, Jalili 2020). The evaluation of the impact of land use and land cover changes on the water quality of the Malacca River in the Southwest Peninsular Malaysia exhibited that TSS and EC had caused a decrease in the river water quality in the areas with agricultural activities (Hua 2017; Sajjadi *et al.* 2019). Studies on the Sarapuí River in southeastern Brazil revealed that agricultural land had led to unfavorable water quality (Ebadati 2017; Mello *et al.* 2018). The GIS data improves over time in terms of spatial and temporal resolution. Therefore, they enable a more accurate investigation of suspended sediment concentration for large rivers compared to conventional sampling methods at hydrometric stations, especially in basins with a low density of stations. According to the findings obtained in the present study and studies in other parts of the world, it can be concluded with high certainty that using various fertilizers in agricultural lands leads to the deteriorated quality of the outflow. On the other hand, these lands have a higher ability to be eroded, and because sediments are the cause of pollution transfer, this feature exacerbates the negative impact of this land use class on water quality. In a study, the impact of land use and land cover was investigated on river water quality using water quality index and remote sensing techniques in the Buriganga, Dhaleshwari, Meghn and Padma rivers in Bangladesh. The results revealed that the water quality had a substantial positive correlation with agricultural land and a significant negative association with the built-up area (Gani *et al.* 2023). A study about the quality of the Upper Ganges River in northern India revealed that anthropogenic activities had a strong impact on water quality (Maurya *et al.* 2021). It has been shown that the water quality of large rivers is a reflection of the cumulative effects of anthropogenic activities (such as urban, industrial and agricultural activities, increased consumption of water resources) and natural processes such as precipitation and temperature changes, erosion, weathering of crustal materials (Xiong 2022).

CONCLUSION

The findings of the present study suggested Landsat 8 image data as a highly useful tool for monitoring changes in river water quality. This is important in several ways. First, it is impossible to continuously monitor the concentration of WQPs in many sediment monitoring stations in Iran. Especially in flood conditions and high flows, it is far unlikely to monitor the concentration of suspended sediments due to technical limitations and sampling costs. Therefore, satellite data, due to the increasing progress and development of this technology, makes it possible to monitor suspended sediments with appropriate time resolution. For example, Landsat satellites make it possible to image a certain area every 16 days on average. Second, even if it is possible to remove the technical limitations for sampling quality parameters from rivers during floods, the sampling operation will still incur costs for the trustees. Therefore, free access to satellite data sources today can be fruitful in order to reduce current costs. Third, there are no hydrometric stations in many watersheds of Iran, especially in distant and mountainous areas. Therefore, satellite images can be used to develop algorithms for estimating the concentration of suspended sediments in watersheds with sediment monitoring stations, and the regression equations obtained from these algorithms can be extended to the areas without land sediment monitoring data.

REFERENCES

Ansari, M & Akhoondzadeh, M 2020, Mapping water salinity using Landsat-8 OLI satellite images (Case study: Karun basin located in Iran). *Advances in Space Research*, 65: 1490-1502.

Bihamta, MR & Zare Chahouki, MA 2015, Principles of statistics for the natural resources science. University of Tehran Press, Tehran, Iran.

Cerqueira, TC, Mendonça, RL, Gomes, RL, de Jesus, RM & da Silva, DML 2020 Effects of urbanization on water quality in a watershed in northeastern Brazil. *Environmental Monitoring and Assessment*, 192: 65-73.

Clay Barrett, D & Frazier, A 2016, Automated method for monitoring water quality using Landsat imagery. *Water*, 8: 257-269.

Ebadati, N 2017 Statistical analysis of Dez River water quality, Southwest Iran. *Anthropogenic Pollution*, 1: 46-60

Fensholt, R, Sandholt, I & Pround, SR 2010, Assessment of MODIS sun-sensor geometry variations effect on observed NDVI using MSG SEVIRI geostationary data. *International Journal of Remote Sensing*, 31: 6163-6187.

Gani, MA, Sajib, AM, Siddik, MA & Moniruzzaman, M 2023, Assessing the impact of land use and land cover on river water quality using water quality index and remote sensing techniques. *Environmental Monitoring and Assessment*, 195: 449-557.

Ghaffari, A, Nasseri, M & Pasebani Someeh, A 2022, Assessing the economic effects of drought using Positive Mathematical Planning model under climate change scenarios. *Heliyon*, 8: 11941.

Goodarzi, M, Pourhashemi, M & Azizi, Z 2019, Investigation on Zagros Forests cover changes under the recent droughts using satellite imagery. *Journal of Forest Science*, 65: 9-17.

Gu, Q, Hu, H, Ma, L, Sheng, L, Yang, S, Zhang, X & Chen, L 2019, Characterizing the spatial variations of the relationship between land use and surface water quality using self-organizing map approach. *Ecological Indicators*, 102: 633-643.

Hashemifard, A, Kardavani, P & Asadian, F 2018, Evaluation of Eco-geomorphology and anthropogenic factors role on Karun River water quality (between Gotvand dam to Ahwaz). *Iranian Water Research*, 12: 51-59.

Hua, AK 2017, Land use land cover changes in detection of water quality: A study based on remote sensing and multivariate statistics. *Journal of Environmental and Public Health*, 7515130: 1-12.

Im, J, Jensen, J & Tullis, J 2008 Object-based change detection using correlation image analysis and image segmentation. *International Journal of Remote Sensing*, 29: 399-423.

Jalili, S 2020, Water Quality Assessment Based on HFB I& BMWP Index in Karoon River, Khouzestan Provience (Northwest of Persian Gulf). *Anthropogenic Pollution*, 4: 36-49.

Jalalzadeh, A, Rabieifar, HR, Vosoughifar, H, Razmkhah, A & Fataei, E 2022, Investigation of daily waste load allocation in Zarrineh-rud river for environmental management of cold-water fish species. *Anthropogenic Pollution*, 6: 36-46.

Kändler, M, Blechinger, K, Seidler, C, Pavlů, V, Šanda, M, Dostál, T & Štich, M 2017, Impact of land use on water quality in the upper Nisa catchment in the Czech Republic and in Germany. *Science of The Total Environment*, 586: 1316-1325.

Kavzoglu, T & Colkesen, I 2009, A Kernel function analysis for support vector machines for land cover classification. *International Journal of Applied Earth Observation and Geoinformation*, 11: 352-359.

Liao, K, Xu, S, Wu, J & Zhu, L 2014, Using support vector machines to predict cation exchange capacity of different soil horizons in Qingdao City, China. *Journal of Plant Nutrition Soil Science*, 177: 775-782.

Lim, J & Choi, M 2015, Assessment of water quality based on Landsat 8 operational land imager associated with human activities in Korea. *Environmental Monitoring Assesessment*, 187(6): 384

Luo, Z, Shao, Q, Zuo, Q & Cui, Y 2020, Impact of land use and urbanization on river water quality and ecology in a dam dominated basin. *Journal of Hydrology*, 584: 124655.

Mishra, AP, Khali, H, Singh, S, Pande, CB, Singh, R & Chaurasia, SK 2021, An assessment of in-situ water quality parameters and its variation with Landsat 8 Level 1 Surface Reflectance datasets. *International Journal of Environmental Analytical Chemistry*, pp. 1-23. DOI: 10.1080/03067319.2021.1954175

Mello, KD, Valente, RA, Randhir, TO, dos Santos, ACA & Vettorazzi, CA 2018, Effects of land use and land cover on water quality of low-order streams in Southeastern Brazil: Watershed versus riparian zone. *CATENA*, 167: 130-138.

Markogianni, V, Kalivas, D, Petropoulos, GP & Dimitriou, E 2018, An appraisal of the potential of Landsat 8 in estimating chlorophyll-a, ammonium concentrations and other water quality indicators. *Remote Sensing*, 10: 1-22.

Maynard, JJ, Karl, JW & Browning, DM 2016, Effect of spatial image support in detecting long-term vegetation change from satellite time-series. *Landscape Ecology*, 31: 2045-2062.

Maurya, PK, Ali, SA, Alharbi, RS, Yadav, KK, Alfaisal, FM, Ahmad, A, Ditthakit, P, Prasad, S, Jung, YK & Jeon, BH 2021, Impacts of land use change on water quality index in the Upper Ganges River near Haridwar, Uttarakhand: A GIS-based analysis. *Water*, 13:3572.

Mushtaq, F & Nee Lala, MG2017, Remote estimation of water quality parameters of Himalayan Lake (Kashmir) using Landsat 8 OLI imagery. *Geocarto International*, 32: 274-285.

Obaid, AA, Ali, KA Abiye, TA & Adam, EM 2021, Assessing the utility of using current generation high-resolution satellites (Sentinel 2 and Landsat 8) to monitor large water supply dam in South Africa. *Remote Sensing Applications: Society and Environment*, 22: 100521.

Office of Operation and Maintenance of Irrigation and Drainage Networks 2017, Water resources in Sefidrud irrigation and drainage network. Guilan Regional Water Authority, Rasht, Iran.

Pizani, F, Maillard, P, Ferreira, A & Amorim, C 2020, Estimation of water quality in a reservoir from Sentinel-2 MSI and Landsat-8, OLI. *Sensors*, V-3-2020, 401-408.

Pushparaj, J & Hegde, AV 2017, Evaluation of pan-sharpening methods for spatial and spectral quality. *Applied Geomatics*, 9: 1-12.

Quang, NH, Dinh, NT, Dien, NT & Son, LT 2023, Calibration of Sentinel-2 Surface Reflectance for water quality modelling in Binh Dinh's Coastal Zone of Vietnam. *Sustainability*, 15:2-20.

Sarp, G 2014, Spectral and spatial quality analysis of pan-sharpening algorithms: A case study in Istanbul. *European Journal of Remote Sensing*, 47:19-28.

Safizadeh, E, Karimi, D, Gahfarzadeh, HR & Pourhashemi, SA 2021, Investigation of physicochemical properties of water in downstream areas of selected dams in Aras catchment and water quality assessment (Case study: Aras catchment in the border area of Iran and Armenia). *Anthropogenic Pollution*, 5: 41-48.

Sajjadi, N, Davoodi, M, & Jozi, S 2019, The quality assessment of Kan River's resources in terms of agricultural and drinking purposes. *Anthropogenic Pollution*, 3: 46-53.

Shukla, AK, Ojha, CSP, Mijic, A, Buytaert, W, Pathak, S, Garg, RD & Shukla S.2018, Population growth, land use and land cover transformations, and water quality nexus in the Upper Ganga River basin. *Hydrology and Earth System Sciences*, 22: 4745-4770.

Tian, Y, Jiang, Y, Liu, Q, Dong, M, Xu, D, Liu, Y & Xu, X 2019, Using a water quality index to assess the water quality of the upper and middle streams of the Luanhe River, northern China. *Science of The Total*

Environment, 667: 142-151.

Vakili, T & Amanollahi, J 2020, Determination of optically inactive water quality variables using Landsat 8 data: A case study in Geshlagh reservoir affected by agricultural land use. *Journal of Cleaner Production*, 247: 119134.

Xiong, F, Chen, Y, Zhang, S, Xu, Y, Lu, Y, Qu, X, Gao, W, Wu, X, Xin, W, Gang, DD & Lin, LS 2022, Land use, hydrology, and climate influence water quality of China's largest river. *Journal of Environmental Management*, 318: 115581.

Xu, S & Ehlers, M 2017, Hyperspectral image sharpening based on Ehlers Fusion, International Archives of the Photogrammetry. *Remote Sensing and Spatial Information Sciences*, XLII-2/W7: 941-947.

Xu, H 2006, Modification of normalized difference water index (NDWI) to enhance open water features in remotely sensed imagery. *International Journal of Remote Sensing*, 27: 3025-3033.

Yadav, S, Babel, MS, Shrestha, S & Deb, P 2019, Land use impact on the water quality of large tropical river: Mun River Basin, Thailand. *Environmental Monitoring and Assessment*, 191: 614-618.

Yia, L, Binga, L, Qian-lia, L, Chenc, P & Yuana, L 2012, A change detection method for remote sensing image based on Multi-Feature Differencing Kernel Svm, ISPRS Annals of Photogrammetry. *Remote Sensing and Spatial Information Sciences*, 1: 227-235

Zhang, JX, Yang, J & Reinartz, P 2016, The optimized block-regression-based fusion algorithm for pan sharpening of very high-resolution satellite imagery, The International Archives of the Photogrammetry, *Remote Sensing and Spatial Information Sciences*, XLI-B7: XXIII ISPRS Congress, pp. 12-19.

Zhang, Z, Zhang, Du, J, Chen, D & Zhang, W 2021, Impacts of land use at multiple buffer scales on seasonal water quality in a reticular river network area, *PLoS ONE*, 16: e0244606.

Bibliographic information of this paper for citing:

Pourhabib, Y, Fataei, E, Nasehi, F, Khanizadeh, B, Saadati, H 2025, Monitoring the spatial changes of river water quality through the fusion of Landsat 8 images and statistical models (A case study: Sefidroud River, Northwest Iran), Caspian Journal of Environmental Sciences, 23: 315-326.